# A simplified method for design of geosynthetic tubes

Guo, Wei; Chu, Jian; Nie, Wen; Yan, Shuwang

2014

Guo, W., Chu, J., Nie, W., & Yan, S. (2014). A simplified method for design of geosynthetic tubes. Geotextiles and Geomembranes, in press.

https://hdl.handle.net/10356/105790

https://doi.org/10.1016/j.geotexmem.2014.06.006

# A Simplified Method for Design of Geosynthetic Tubes

Wei Guo[1], Jian Chu[2*], Wen Nie[1], Shuwang Yan[3]

[1] School of Civil & Environmental Engineering, Nanyang Technological University, Blk N1, 50 Nanyang Ave, Singapore, 639798.
[2] Department Civil, Construction & Environmental Engineering, Iowa State University, 328 Town Engineering Building, Ames, IA, USA, 50011.
[3]Geotechnical Research Institute, School of Civil Engineering, Tianjin University, 92 Weijin Road, Nankai District, Tianjin, China
[*]Corresponding author, E-mail: jchu@iastate.edu, Tel: 515-294-3157, Fax: 515-294-8216

**ABSTRACT:**

A simplified method for the design of impermeable geosynthetic tubes inflated using liquid is proposed in this paper. Adopting a computer program for an existing theoretical model, relationships between pumping pressure and geometric parameters for geosynthetic tubes can be established. A set of simplified dimensionless design equations are then derived using the Chapman-Richard curve fitting method. The validity of this simplified method was verified using other established methods and laboratory model tests. The proposed simplified method can thus be used for routine or preliminary design.

**Keywords:** Geosynthetic tube; Curve Fitting; Chapman-Richard Model

## 1. Introduction

Geotextile tubes have been widely used for various engineering applications, such as breakwaters and beach restoration projects (Leshchinsky et al., 1996; Shin and Oh, 2007; Lawson, 2008; Cantré and Saathoff, 2011; Yan and Chu, 2010; Chu et al., 2012; Yee et al., 2012; Yee and Lawson, 2012; Lee and Douglas, 2012). However, the design of geotextile tubes is still not a straight forward task. Several analytical solutions for the liquid filled geosynthetic tubes resting on rigid foundation have been proposed by Leshchinsky et al., (1996), Plaut and Suherman (1998), Guo et al. (2011), and Cantré and Saathoff (2011). Most of these solutions are based on the assumptions that the tube is long enough to be simplified into a plane-strain problem, the friction between geosynthetic and internal water are

neglectable and the tubes are resting on a rigid base. As there is no close-form solution for the proposed theories, all the above analytical solutions require the running of computer programs. This is not convenient for preliminary design where some trial and error processes or parametric studies are involved in the selection of the dimensions of the geosynthetic tubes and types of geotextiles to be used. The alternative method is to use design charts (Guo et al. 2014). However, the accuracy of using design charts is not always satisfactory.

Another simplification method is to use curve fitting which is presented in this paper. An analytical model (Guo et al. 2011) was used to generate dimensionless design charts. Then the Chapman-Richard method was adopted to derive best-fit equations for these curves. These best-fit equations form a simplified method which was verified using other established analytical solutions and laboratory model tests. As the equations so derived are dimensionless, theoretically they should be applicable to any design situation. In this paper, only solutions for impermeable geosynthetic tubes filled with uniform liquid is proposed. However, these solutions may also be used to a permeable geotextile tube at where the tube is inflated to its fullest by assuming that the dewatering during filling period is neglectable. It should also be pointed out that the proposed curve fitting method may not be suitable to cases when geosynthetic tubes are partially or fully submerged by external water.

## 2. Analytical solution adopted

The analytical solution proposed by Guo et al (2011) was adopted to derive relationships between pumping pressure and geometry parameters. In the solution by Guo et al. (2011) the following assumptions are adopted, (1) the geosynthetic tube is sufficiently long to be assumed into a plane strain problem; (2) the geosynthetic sheet is thin, flexible so that its weight and extension can be neglected; (3) the friction between the geosynthetic tube and the fill material, or that between the geosynthetic tube and the rigid foundation are neglected. Some of the above hypotheses are also made in the exiting theoretical solutions such as Leshchinsky et al. (1996), Plaut and Suherman (1998), Cantré (2002), Cantré and Saathoff (2010), Guo et al. (2014). This solution (Guo et al, 2011) is proposed for a geosynthetic tube inflated by liquid with uniform unit weight, $\gamma$. The free body diagram of a half cross-section

of the tube is plotted in Fig. 1(a). The height and width of the cross-section of the geosynthetic tube are written as $H$ and $B$, respectively. The contact width between the tube and the subgrade is $b$. The tensile force along the geosynthetic tube per unit length is defined as $T$. The forces acting on the free body along the horizontal direction involve the hydraulic force and the tensile force. The forces equilibrium along the horizontal direction yields the expression of tensile force as shown in Eq. (1). A free body diagram of a section from point $O$ to a point $S(x, y)$ on the cross-section is selected for force equilibrium analysis as shown in Fig. 1(b). The angle between the tangent direction at point S($x$, $y$) and the $x$ axis is denoted as $\theta$. The forces acting along the horizontal direction could solve the expression of sin $\theta$, $x$ and $y$ as shown in Eq. (2), (3) and (4), respectively. Factor $Q$ in Eq. (4) is a non-dimensional factor related to pumping pressure which can be calculated by Eq. (5).

$$T = (p_0 H + \frac{1}{2}\gamma H^2)/2 \tag{1}$$

$$\sin\theta = 1 - (p_0 x + \frac{1}{2}\gamma x^2)/T \tag{2}$$

$$x = \frac{1}{\gamma}\left[-p_0 + \sqrt{p_0^2 + 2\gamma T(1-\sin\theta)}\right] \tag{3}$$

$$y = -\sqrt{\frac{T}{2\gamma}}\int(\sqrt{Q-\sin\theta} - \frac{Q}{\sqrt{Q-\sin\theta}})d\theta \tag{4}$$

$$Q = \frac{1}{2\gamma T}(p_0^2 + 2\gamma T) \tag{5}$$

Given unit weight of fill, $\gamma$, pumping pressure, $p_0$, height of cross-section, $H$, and boundary conditions $x = 0$, $\theta = \pi/2$ and $x = H$, $\theta = -\pi/2$, the cross-section and tensile force can be calculated using Eqs. (1) to (5). As Eq. (5) contains the first and second elliptic integrals and thus has no closed-form solutions, a computer program is needed to solve this equation using the adaptive Runge-Kutta-Merson method (RKM4) (Lukehart, 1963; Christiansen, 1970). The iteration procedure is as follows: (a) input the initial parameters: $\gamma$, $p_0$, $H$; (b) calculate $T$, $Q$, and $\sin\theta$ using Eqs. (1), (2) and (5), respectively; (c) solve Eqs. (3) and (4) to get the cross-section of the filled tube using the RKM4 method. If the perimeter, $L$, is taken as an

input rather than $H$, the iteration can be done by assuming $H_{try} = L/\pi$ for the above steps (a) to (c) to solve the equations and calculate the generated perimeter of cross-section, $L_{try}$. If $L_{try} \neq L$, then modify $H_{try}$ and repeat step (a) to (c) until the difference between generated $L_{try}$ and given $L$ is less than *1.0E-6*.

Using a computer program written for the method by Guo et al. (2011), the relationships between pumping pressure and the geometry of the geosynthetic tubes can be established. Fig. 2 shows the pumping pressures versus height of cross-section curves calculated using different unit weights, $\gamma$, and perimeter, $L$,. For generality, dimensionless parameters, such as the normalized height, $H/L$, and the normalized pumping pressure, $p_0/(\gamma L)$, are used in Fig. 2. As a single curve is obtained for different ranges of parameters, the relationship shown in Fig. 2 can be considered general. Similar relationships between normalized pumping pressure and normalized area, $A/L^2$, normalized width of cross-section, $B/L$, normalized contact width with ground, $b/L$, and normalized tensile force, $T/(\gamma L^2)$, are shown in Figs. 3, 4, 5, and 6, respectively. The normalization method adopted is similar to that by Plaut and Suherman (1998). It should be noted that a range of parameters are adopted as shown in Fig. 2 to testify that these relationships are applicable over a wide range of design situations.

## 3. Curve-fitting Methods

The Chapman-Richard model (Ratkowsky, 1990) is adopted to get best-fit equations for the numerical results presented in Figs. 2 to 6. The mathematical expression of the Chapman-Richard model is shown as,

$$y = \delta(1 - e^{-\mu x})^{\lambda} + \varepsilon \qquad (6)$$

where $\delta$ is the amplitude of the curve, $\varepsilon$ is the offset from zero, $\mu$ and $\lambda$ are rate constants and $e$ is the base of the natural logarithm. The physical meanings of the parameters $\delta$ and $\varepsilon$ are illustrated in Fig. 7. The amplitude of $\delta$ can also be negative value which means $y$ reduces from $\varepsilon$ to $\varepsilon–\delta$ with respect to the increasing of $x$ value as shown in Fig. 7b.

Eq. (6) was adopted to best-fit Figs. 2 to 6. This was carried out using the "Solver" function in the Microsoft Excel program with $\mu$ and $\lambda$ as variables and $R^2$ as objective. The fitted curves and equations are also shown in Figs. 2 to 6. The $R^2$ values for all the curve fittings are above 0.999. In the curve-fitting for Fig. 2, the amplitude value, $\delta$ = 0.318(or $1/\pi$), is calculated by the limit value of $H/L$ (circular cross-section) when $p_0/(\gamma L)$ tends to $+\infty$. The condition $H = 0$ when $p_0 = 0$ (or $\varepsilon = 0$) was used in the calculation. The final relationship between $H$ and $p_0$ can be written as shown in Eq. (7). Similar curve-fitting procedure was adopted for Fig. 3. The equation for the relationship between $p_0$ and $A$ is given in Eq. (8).

$$H = 0.318L(1-e^{-\frac{2.114p_0}{\gamma L}})^{0.188} \quad (7)$$

$$A = 0.08L^2(1-e^{-\frac{6.504p_0}{\gamma L}})^{0.134} \quad (8)$$

To curve-fit the data in Fig. 5, the condition $B = L/2$ or $\varepsilon = 0.5$ when $p_0 = 0$ was used. The width of the cross-section reduces with the increasing of pumping pressure. The limit cross-section when $p_0/\gamma L = +\infty$ is when the tube is in a circular shape where $B/L = 1/\pi$. In another word, the amplitude of the width changing $\delta$ is $(0.5 - 1/\pi)$ or $\delta = 0.1817$ as explained in Fig. 7. The relationship between $B$ and $p_0$ is given in Eq. (9). The same method was adopted to the data shown in Fig. 6. The equation for the relationship between $p_0$ and $b$ are given in Eq. (10).

$$B = 0.5L - 0.1817L(1-e^{-\frac{2.138p_0}{\gamma L}})^{0.204} \quad (9)$$

$$b = 0.5L - 0.5L(1-e^{-\frac{0.937p_0}{\gamma L}})^{0.242} \quad (10)$$

As shown in Fig. 4, a dimensionless relationship between tensile force and pumping pressure can be obtained based on Eq. (1) and Fig. (2). Using this equation, a relationship between T and $p_0$ is given as:

$$T = 0.159 p_0 L(1 - e^{-\frac{2.114 p_0}{\gamma L}})^{0.188} + 0.025 \gamma L^2 (1 - e^{-\frac{2.114 p_0}{\gamma L}})^{0.376} \quad (11)$$

## 4. Design procedure using the curve fitting method

Generally, there are the following three design scenarios depending on the inputs available:

1) When $\gamma$, $L$ and $p_0$ are taken as inputs, the height of the tube, $H$, area, $A$, and width of the cross-section, $B$, contact width with ground, $b$, and tensile force, $T$, can be calculated directly using Eqs. (7), (8), (9), (10) and (11), respectively;
2) When $\gamma$, $L$ and $H$ are taken as inputs, the required pumping pressure, $p_0$, can be calculated using Eq. (7) which can be re-written as:

$$p_0 = -0.473 \gamma L \ln(1 - (\pi \frac{H}{L})^{5.32}) \quad (12)$$

The rest of the designing procedure is the same as that in the first case;
3) When $\gamma$, $H$ and $p_0$ are taken as inputs, the perimeter $L$ cannot be calculated directly using Eq. (7) as there is no closed-from solution. Then an indirectly method to use a build-in function, "Goal Seek", in the Microsoft Excel program is suggested to search a $L$ to meet Eq. (7). After L is obtained, the designing procedure will be the same as that in the first case.

## 5. Verification of the curving fitting method

### 5.1 Comparison with analytical methods

In order to verify the accuracy of the proposed method, the predictions made using the proposed method are compared with the solutions given by other analytical methods. The first comparison is with the method proposed by Leshchinsky et al. (1996). The Leshchinsky et al.'s theory has been encoded to a computer program, GeoCoPS, by Leshchinsky and Leshchinsky (1996) and calibrated against a case with $L = 9\ m$ and $\gamma = 12\ kN/m^3$. For the same case, the results from the proposed method are compared with those from Leshchinsky *et al.* (1996) in Table 1. It can be seen that the differences between the two solutions are less than 5.9%.

The second comparison is with the design charts developed by Cantré (2002) in Figs. 8a and 8b for $p_0/(\gamma L)$ vs $H/L$ and $H/L$ vs $T/(\gamma L^2)$ relationships respectively. The design charts by Cantre (2002) were based on a non-dimensional method proposed by Plaut and Suherman (1998). Using the proposed method, the normalized pumping pressure versus height of geosynthetic tube relationship can be calculated using Eq. (7) and plotted in Figs. 8a. Using Eqs. (1) and (12), a relationship between $T/(\gamma L^2)$ and $H/L$ can be derived as Eq. (14). Eq. (14) was used to plot Fig. 8b. It can be seen from Fig. 8 that very good agreement between the proposed solution and Cantre's (2002) has been achieved.

$$\frac{T}{\gamma L^2} = -0.2365\frac{H}{L}\ln(1-(\pi\frac{H}{L})^{5.32}) + 0.25(\frac{H}{L})^2 \qquad (14)$$

Comparisons of the proposed method with the method by Malík (2009) for impermeable geosynthetic tube resting on rigid foundation are also made for a geosynthetic tube with $L$ = 10 *m* and $\gamma$ = 10 $kN/m^3$ as a case. The $H$ vs $A$ and $H$ vs $T$ curves are plotted in Fig. 9a and 9b, respectively. The Eq. (15) derived from Eq. (8) and (12) was adopted to calculate the area of cross-section. The Eq. (14) was used to calculate the tensile force. The comparisons between the results from the curve fitting equations and those from Malík (2009) are plotted in Figs. 9a and 9b. Good agreements have been obtained.

$$A = 0.08L^2(1-e^{3.0764\ln(1-(\pi H/L)^{5.32})})^{0.134} \qquad (15)$$

**5.2 Comparison with model test results**

The proposed method is also applied to predict the performance of some laboratory large scale model tests. In the model tests, three tubes with dimensions of 1-*m*-wide by 2-*m*-long (model T1), 1.5-*m*-wide by 3-*m*-long (model T2) and 2-*m*-wide by 4-*m*-long (model T3). The geosynthetic tubes were inflated by tap water. The profiles of the geosynthetic tubes were measured by a laser sensor (model ILD1700-750 by Micro-Epsilon Company). The laser sensor hanging on an x-beam made of an aluminum alloy bar could move from left to right. The x-beam was fixed on a frame as shown in Fig. 10. When the laser sensor moved

horizontally along the x-beam, the vertical distance between the laser sensor and the top surface of the geosynthetic tubes was measured and recorded. Before each model test, the distance between the concrete floor and the laser sensor was measured. The vertical position of a point on the surface of the tube was calculated by the distance to the floor subtracting the laser sensor reading. A ruler attached to the x-beam was used to measure the horizontal position of the test points. In order to avoid the influence from the blocked air in the tube, the air in the tube was pumped out using a vacuum pump before the test. More detail of the model test is referred to Guo (2012) or Guo et al. (2013). The testing data of the three model tests are compared with the predictions made by the proposed method in Figs. 11a and 11b for both the normalized height versus normalized pumping pressure and the normalized width versus normalized pumping pressure relationships respectively. It can be seen that good agreement is achieved.

A comparison with the model test results presented by Silvester and Hsu (1997) was also made. In the model tests (Liu, 1978; Silverster and Hse, 1997), the geosynthetic tube was made of plastic and inflated by tap water. In Silvester and Hsu (1997), pressure head in the tube, $b_1$, instead of pumping pressure, and an equivalent diameter of the tube, $D$, were used for data interpretation where $b_1 = p_0/\gamma + H$ and $D = L/\pi$. Those parameters are used for the graphs shown in Figs. 12a and 12b. The corresponding predictions using the proposed method are also shown in Figs. 12a and 12b, respectively. Again good agreement is achieved.

## 6. Conclusions

In this paper, a simplified method for design of impermeable geosynthetic tube resting on rigid foundation is proposed based on curve-fitting of an analytical solution using the Chapman-Richard model. The predictions made by the proposed method were compared with other theoretical solutions and model testing data and good agreements were achieved for all the cases. Thus, the proposed method can be used with a hand-hold calculator for routine or preliminary design. The accuracy of the proposed method is comparable with that offered by other methods where a computer program will have to be used.

## 7. Notations

| | |
|---|---|
| $A$ | Area of cross-section |
| $b$ | Contact width with ground |
| $B$ | Width of cross-section |
| $H$ | Height of cross-section |
| $k$ | Height to width ratio |
| $L$ | Perimeter of cross-section |
| $p_0$ | Pumping pressure |
| $T$ | Tensile force per unit length |
| $\gamma$ | Unit weight of filling slurry |
| $\delta$ | Amplitude of the Chapman-Richard model |
| $\varepsilon$ | Offset from zero of the Chapman-Richard model |
| $\mu, \lambda$ | Constant variables in the Chapman-Richard model |

## 8. References


Cantré, S., (2002). "Geotextile tubes--analytical design aspects". *Geotextiles and Geomembranes*, Vol. 20(5), pp. 305-319.

Cantré, S., and Saathoff, F., (2011). "Design method for geotextile tubes considering strain - Formulation and verification by laboratory tests using photogrammetry". *Geotextiles and Geomembranes*, Vol. 29(3), pp. 201-210.

Christiansen, J., (1970). " Numerical solution of ordinary simultaneous differential equations of the 1st order using a method for automatic step change". *Numerische Mathematik,* 14, pp. 317-324.

Chu, J., Guo, W. and Yan, S. W., (2011). "Geosynthetic Tubes and Geosynthetic Mats: Analyses and Applications". *Geotechnical Engineering*, 42(1), 56-65.

Chu, J., Yan, S. W. and Li, W., (2012). Innovative methods for dike construction– An overview, *Geotextiles and Geomembranes* 30, 35-42.

Guo, W., (2012). "Geosynthetic Tubes and Mats: Experimental and Analytical Studies". *Ph.D. Thesis*, Nanyang Technological University, Singapore.

Guo, W., Chu, J. and Yan, S. W., (2011), "Effect of subgrade soil stiffness on the design of geosynthetic tube*".Geotextiles and Geomembranes*, 29(3), 277-284.

Guo W., Chu J., Yan S.W. (2013). "Recent studies of geosynthetic tubes and geosynthetic mats: an overview". *Geotechnical Engineering*, Vol 44 (4), 115-124.

Guo, W., Chu, J., Yan, S. W. and Nie, W., (2013). "Geosynthetic mattress: analytical solution and verification". *Geotextiles and Geomembranes*, 37, 74-80.

Guo, W., Chu, J., Yan, S. W. and Nie, W. (2014). "Analytical solutions for geosynthetic tube resting on rigid foundation". *Geomechanics and engineering*, 6(1), 65-77.

Guo, W, Chu, J. and Nie, W., (2014). "Analysis of geosynthetic tubes inflated by liquid and onsolidated soil", *Geotextiles and Geomembranes*, http://dx.doi.org/10.1016/j.geotexmem.2014.05.001

Lawson, C.R., (2008). Geotextile containment for hydraulic and environmental engineering, Geosynthetics International, 15(6), 384 – 427.

Lee, E. C. and Douglas, R. S., (2012). Geotextile tubes as submerged dykes for shoreline management in Malaysia. *Geotextiles and Geomembranes* 30: 8-15.

Leshchinsky, D., Leshchinsky, O., Ling, H. I. and Gilbert, P. A. (1996). "Geosynthetic tubes for confining pressurized slurry: some design aspects". *Journal of Geotechnical Engineering*, 122(8), 682-690.

Leshchinsky, D. and Leshchinsky, O. (1996). "Geosynthetic Pressurized Slurry (GeoCoPS): Supplemental Notes for Version 1.0". *Technical Report CPAR-GL-96-1*, US Army Corps of Engineers Waterways Experiment Station, Vicksburg, MS.

Liu, G. S., (1978). "Mortar sausage units for coastal defense". *Master Thesis*, University of Western Australia, Australia.

Lukehart, P. M. (1963). "Algorithm 218. Kutta Merson". *Comm. Assoc. Comput Mach.*, 6(12), 737-738.

Malík, J. (2009). "Some problems connected with 2D modeling of geosynthetic tubes." *Nonlinear Analysis: Real World Applications*, 10(2), pp. 810823.

Plaut, R. and Suherman, S. (1998), "Two-dimensional analysis of geosynthetic tubes", *Acta Mechanica*, 129(3), 207-218.

Ratkowsky, D.A. (1990) "*Handbook of nonlinear regression models*". Marcel Dekker, New York.

Shin, E.C., Oh, Y.I., (2007). Coastal erosion prevention by geotextile tube technology. *Geotextiles and Geomembranes*, 25(4-5): 264-277.

Silvester, R., and Hsu, J.R.C., (1997). "*Coastal stabilization*", Technology & Engineering, 578p.

Yan, S.W. and Chu, J. (2010), "Construction of an offshore dike using slurry filled geotextile mats", *Geotextiles and Geomembranes*, 28, 422-432.

Yee, T.W., Lawson, C.R., Wang, Z.Y., Ding, L., and Liu, Y., (2012). Geotextile tube dewatering of contaminated sediments, Tianjin Eco-City, China. *Geotextiles and Geomembranes* 31, 39-50.

Yee T. W. and Lawson C. R., (2012). Modelling the geotextile tube dewatering process, *Geosynthetics International* 19(5), 339 –353.

Table 1 Comparison of the results calculated from the curve fitting equations with that from Leshchinsky *et al.* (1996) (For $L = 9\ m$, $\gamma = 12\ kN/m^3$)

| $p_0(kPa)$ | Source | $H\ (m)$ | | $B\ (m)$ | | $A\ (m^2)$ | | $T\ (kN/m)$ | |
|---|---|---|---|---|---|---|---|---|---|
| | | Values | Diff(%) | Values | Diff(%) | Values | Diff(%) | Values | Diff(%) |
| 4.8 | Leshchinsky | 1.80 | 1.04 | 3.60 | -2.84 | 5.56 | -3.16 | 14.60 | -2.89 |
| | Curve Fitting | 1.82 | | 3.50 | | 5.38 | | 14.18 | |
| 6.9 | Leshchinsky | 2.00 | -3.01 | 3.64 | -5.90 | 5.76 | -2.64 | 18.10 | -1.35 |
| | Curve Fitting | 1.94 | | 3.43 | | 5.61 | | 17.86 | |
| 34.5 | Leshchinsky | 2.50 | 0.15 | 3.21 | -3.95 | 6.45 | -1.32 | 61.70 | 0.14 |
| | Curve Fitting | 2.50 | | 3.08 | | 6.36 | | 61.79 | |
| 52.4 | Leshchinsky | 2.60 | 1.26 | 3.13 | -4.01 | 6.51 | -1.04 | 87.50 | 2.33 |
| | Curve Fitting | 2.63 | | 3.00 | | 6.44 | | 89.54 | |
| 103.5 | Leshchinsky | 2.70 | 3.22 | 3.00 | -3.00 | 6.57 | -1.40 | 162.00 | 3.25 |
| | Curve Fitting | 2.79 | | 2.91 | | 6.48 | | 167.26 | |
| 122.8 | Leshchinsky | 2.70 | 4.13 | 2.96 | -2.19 | 6.57 | -1.38 | 189.70 | 3.36 |
| | Curve Fitting | 2.81 | | 2.90 | | 6.48 | | 196.07 | |

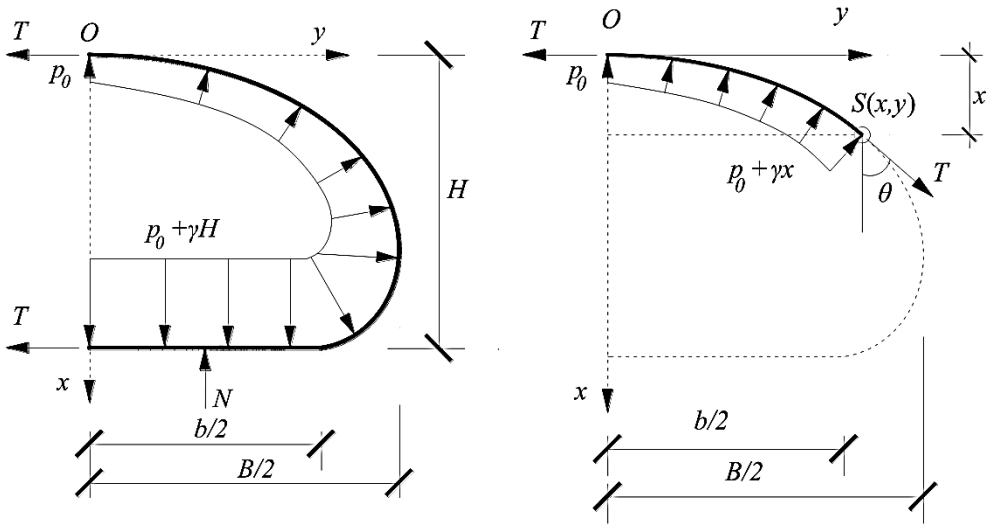


(a) Free body of half cross-section (b) Free body of calculated curve OS

Fig. 1 Free body diagrams of geosynthetic tube resting on rigid foundation

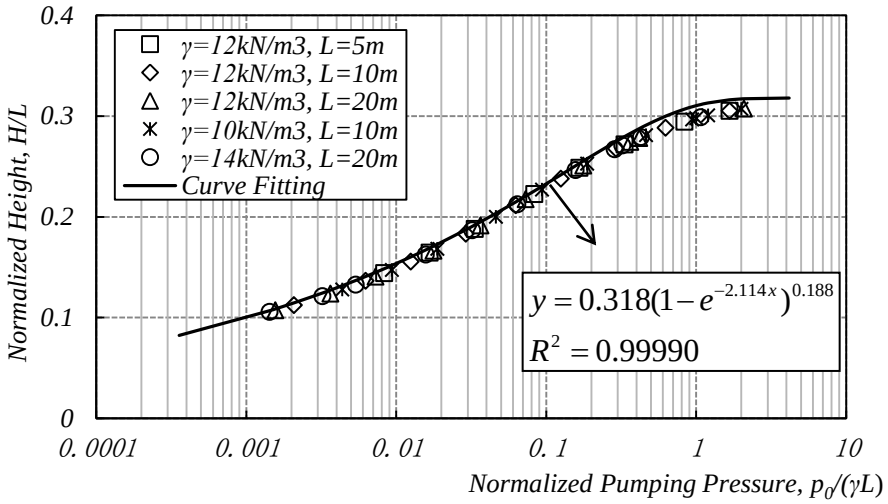


Fig. 2 Curve fitting for the relationship between $p_0/(\gamma L)$ and $H/L$

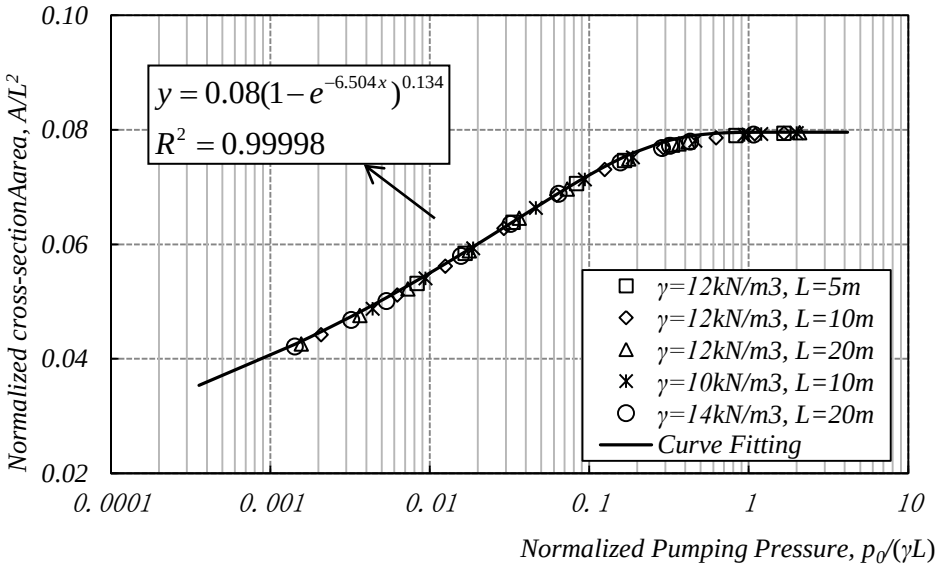


Fig. 3 Curve fitting for the relationship between $p_0/(\gamma L)$ and $A/L^2$

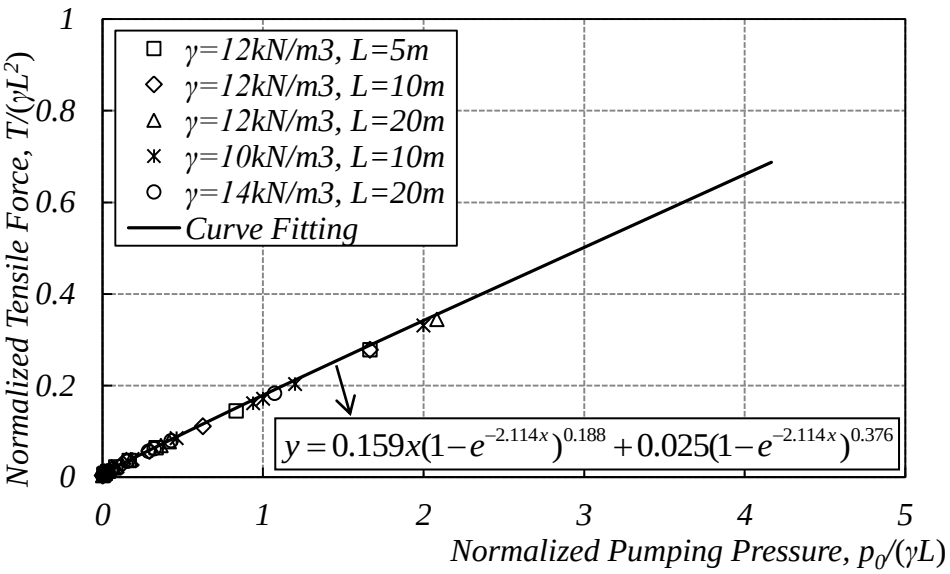


Fig. 4 Curve fitting for the relationship between $p_0/(\gamma L)$ and $T/\gamma L^2$

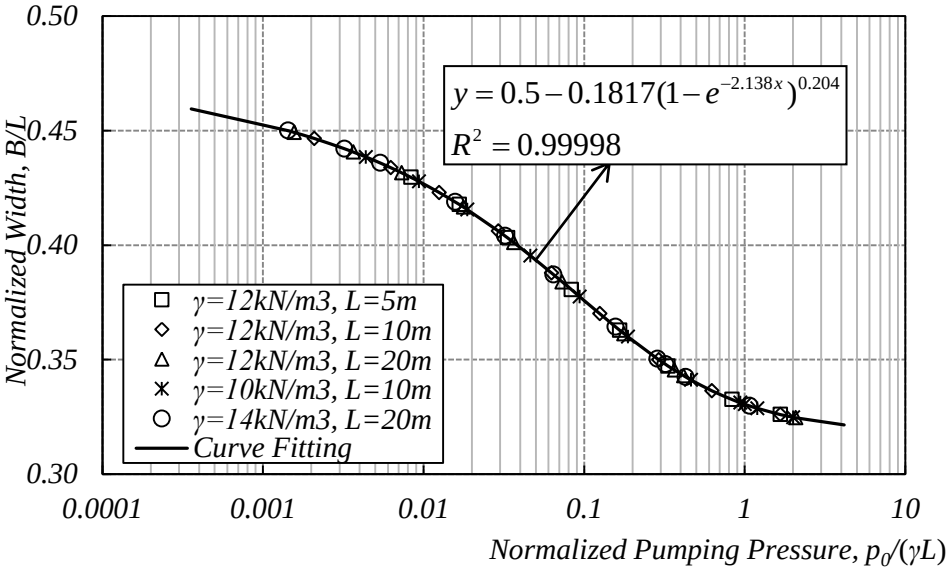


Fig. 5 Curve fitting for the relationship between $p_0/(\gamma L)$ and $B/L$

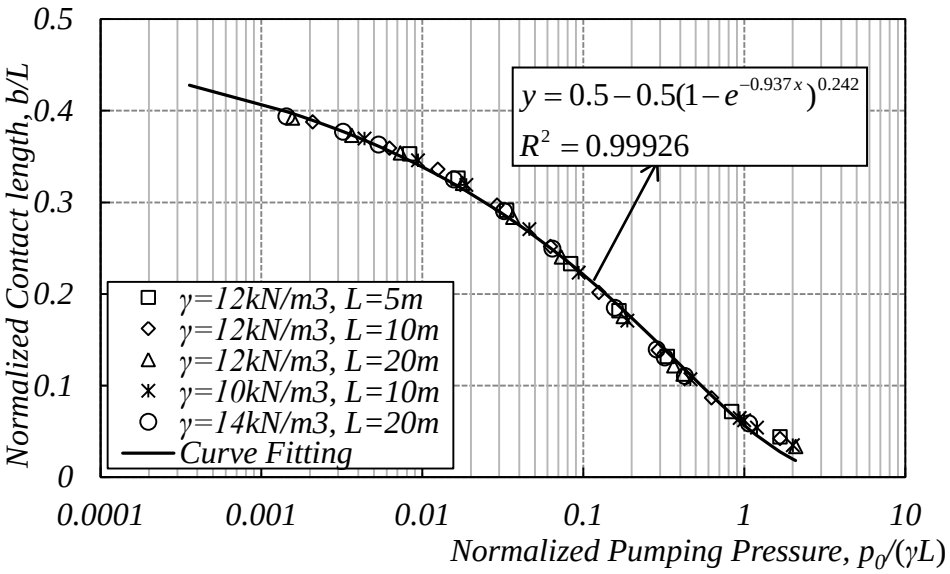


Fig. 6 Curve fitting for the relationship between $p_0/(\gamma L)$ and $b/L$

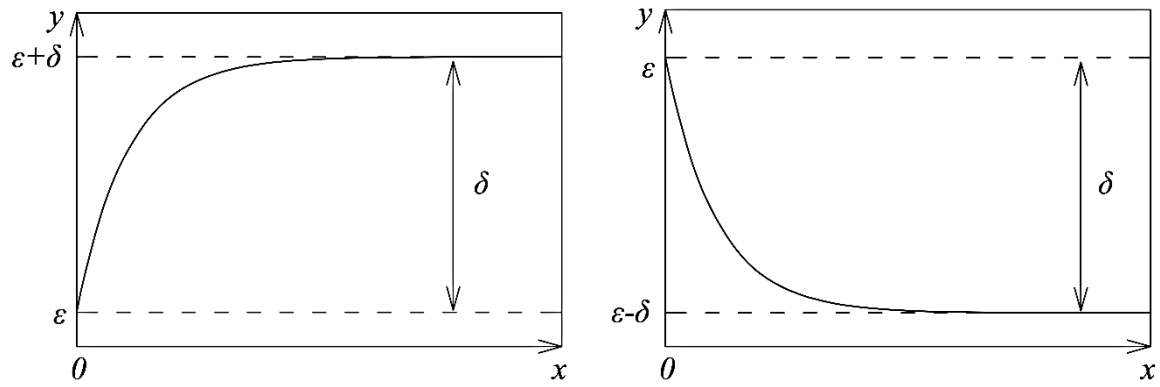


(a) δ > 0 (b) δ < 0

Fig. 7 Illustration of Chapman-Richard model

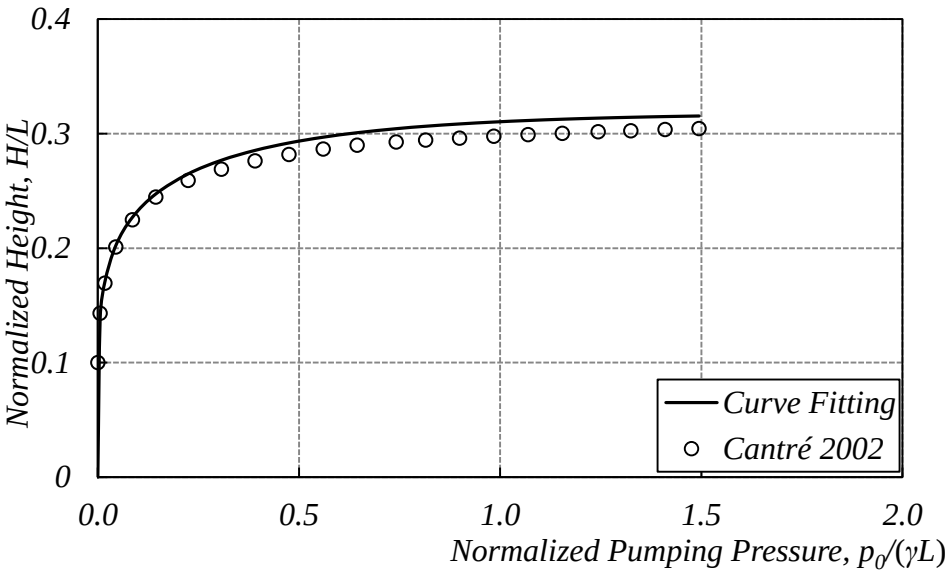


(a) Comparison of $p_0/(\gamma L)$ vs $H/L$ curves

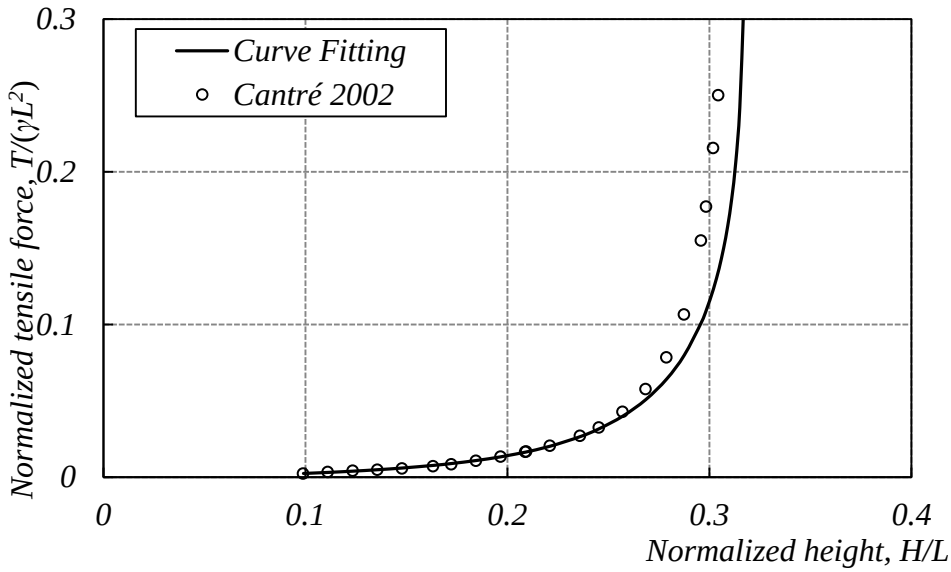


(b) Comparison of $H/L$ vs $T/(\gamma L^2)$ curves

Fig. 8 Comparisons of the results obtained from proposed method and Cantré (2002)

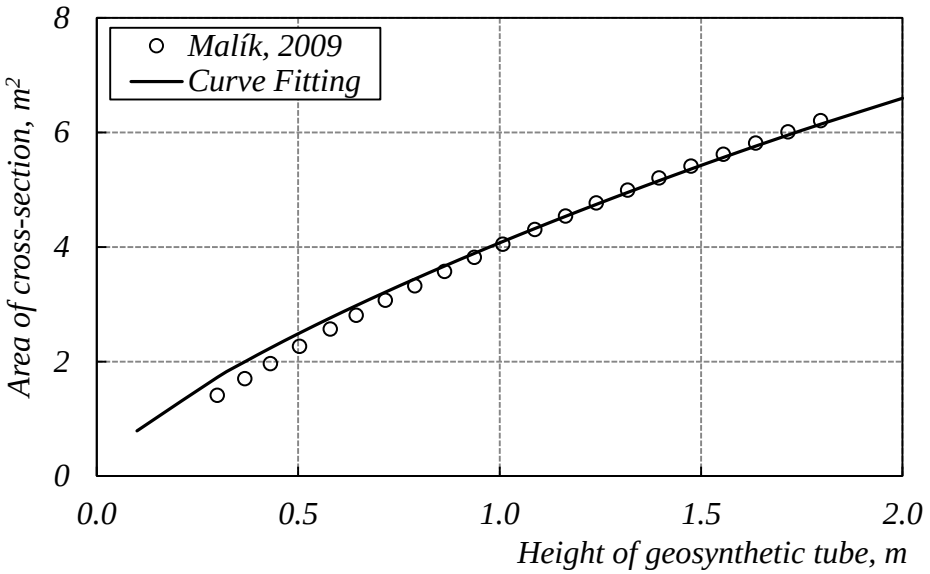


(a) Comparison of $H$ vs $A$ curves

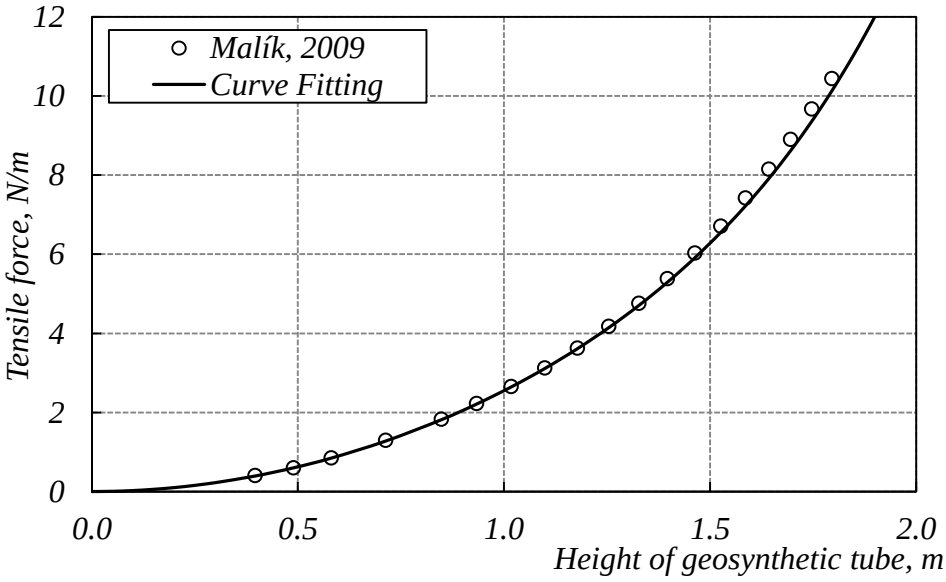


(b) Comparison of $H$ vs $T$ curves

Fig. 9 Comparisons of the results obtained from proposed method and Malík (2009)

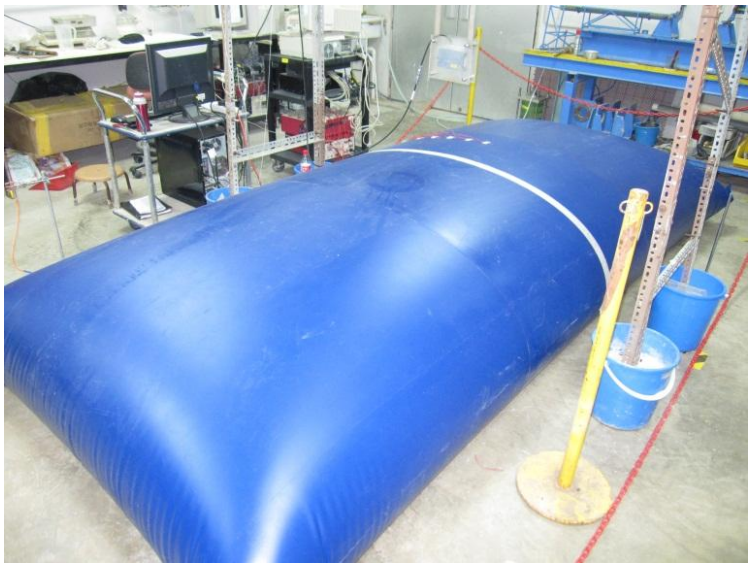

(a) Photo of model T3 after filled by tap water

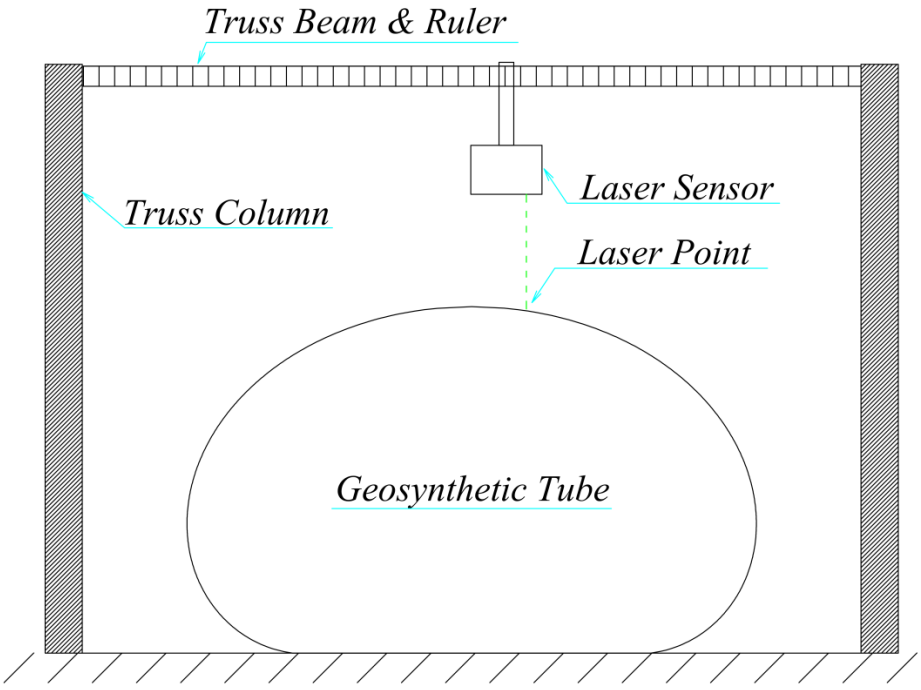


(b) Sketch of the model test set-up

Fig. 10 Model test set-up

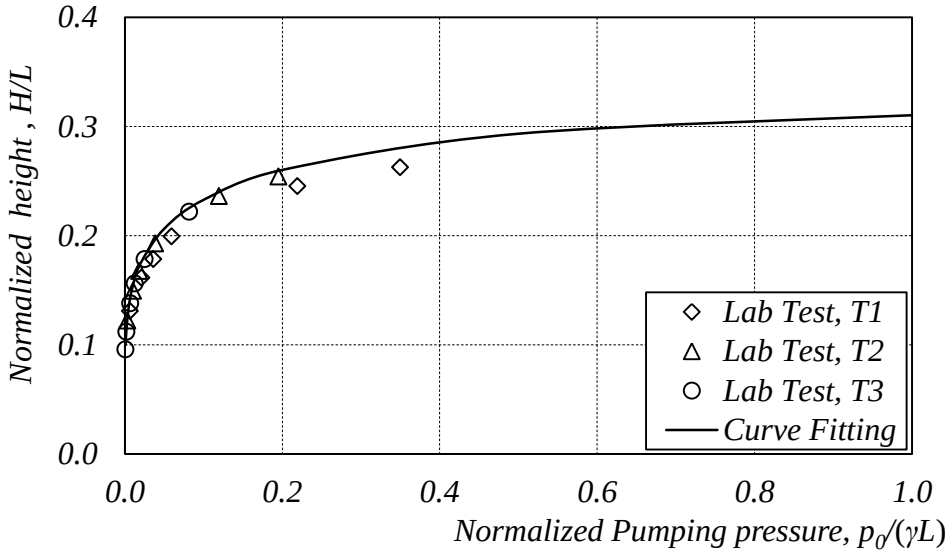


(a) $p_0/(\gamma L)$ vs $H/L$ curves

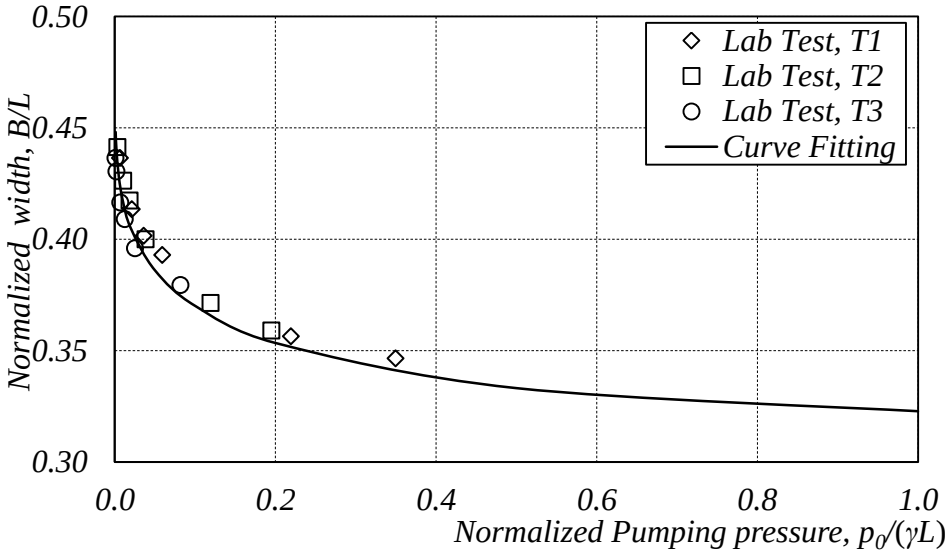


(b) $p_0/(\gamma L)$ vs $B/L$ curves

Fig. 11 Comparisons of the results from proposed method and lab model tests

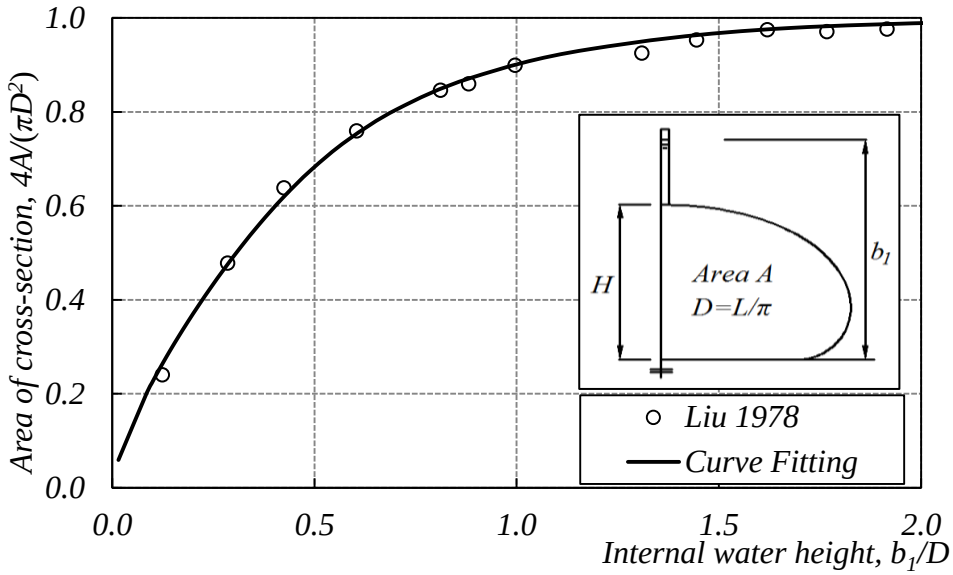


(a) $b_1/D$ vs $4A/\pi D^2$ curves

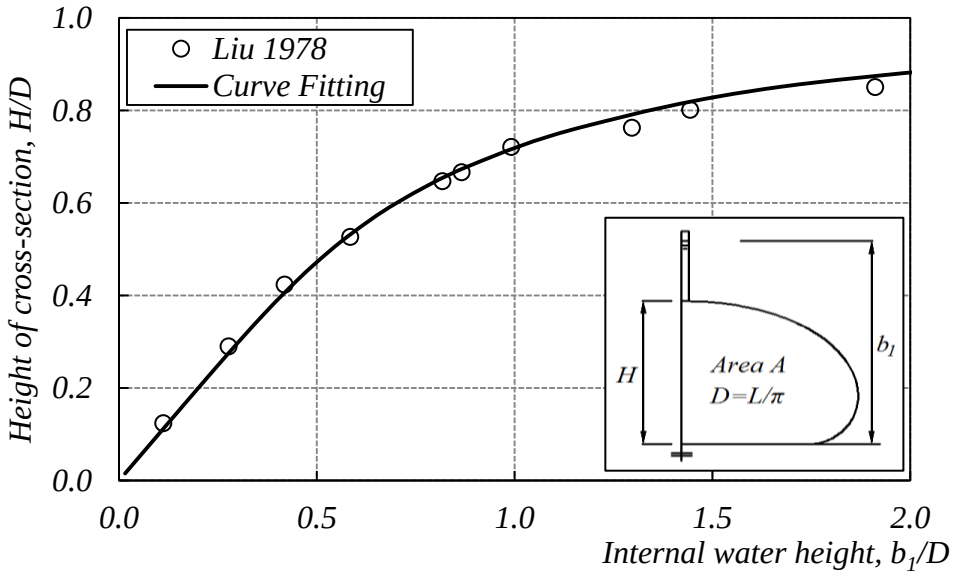


(b) $b_1/D$ vs $H/D$ curves

Fig. 12 Comparisons of the results obtained from proposed method and lab model tests carried out by Silvester and Hsu (1997)